

Nucleation of Embryos of a Second Phase by Individual Impurity Atoms

Matthew O. Zacate, Gary S. Collins, and Luke S.-J. Peng

Washington State University, Department of Physics, Pullman, WA 99164-2814, USA

Abstract

Perturbed angular correlation of gamma rays (PAC) was used to monitor the atomic environments of indium atoms in Ni-Al alloys at temperatures and compositions in the two-phase field between Ni_2Al_3 and NiAl. In earlier PAC measurements at room temperature, the fraction of signal that is characteristic of the Ni_2Al_3 phase greatly exceeded the fraction predicted by the lever-rule, and it was suggested that indium could nucleate small embryos of the Ni_2Al_3 phase in the NiAl single-phase field. Measurements at elevated temperatures are now reported. PAC signals from the Ni_2Al_3 phase are observed to extend into the NiAl single-phase field from 0.5 to 1.0 at.% beyond published phase boundaries that were established by experiments on samples prepared similarly to those in this study. Thus, the new observations support the hypothesis that individual solute atoms can nucleate small crystals of a second phase within a single-phase field. In addition, phase boundaries were calculated from the PAC data, assuming that the lever rule was obeyed, and compared with boundaries from the literature.

1. Introduction

Phase separation generally occurs via heterogeneous nucleation and growth, and extended defects are usually considered as nucleation centers. Can a single impurity atom act as a nucleation center? When an impurity atom in a binary alloy attracts structural vacancies, the arrangement of vacancies around the impurity may closely resemble that of a second phase of the alloy. Under favorable conditions, relaxation around an impurity/vacancy complex may result in a small, localized embryonic crystal of the second phase. If very small, embryos would be difficult to detect using standard macroscopic methods. They could be detected using a spectroscopic technique that has atomic scale resolution and focuses on the solute atoms.

The Ni_2Al_3 -NiAl system has qualities that might be favorable for the formation of Ni_2Al_3 embryos around indium solute atoms in the NiAl phase. The Ni_2Al_3 structure is derived from the NiAl structure by the condensation of Ni-vacancies on every third

<111> plane [1]. This results in two inequivalent Al-sites, one of which has one empty and one filled adjacent Ni-planes and the other of which has two filled adjacent Ni-planes. Indium substitutes for Al in both phases. In Ni-poor NiAl, indium atoms attract and bind multiple vacancies to form indium-vacancy complexes with configurations that are distinguishable using PAC [2,3,4,5]. Two of these defect complexes have vacancies in the first neighbor shell of indium atoms in the same geometries as the inequivalent Al-sites in Ni₂Al₃. Thus, indium in Ni-poor NiAl aggregates vacancies in arrangements that are characteristic of Ni₂Al₃, so that a relaxation in the lattice around the defect complex could induce the Ni₂Al₃ structure locally.

To relate the distribution of indium between the Ni₂Al₃ and NiAl phases to the macroscopic volume fractions of the two phases, consider the change in internal energy of the NiAl phase, E_{11} , and the change in energy of Ni₂Al₃, E_{23} , when indium substitutes for aluminum in the respective phases. It is energetically more favorable for indium to be in the Ni₂Al₃ phase when $E_{23} < E_{11}$, and an expression for the ratio of the fraction of probes in Ni₂Al₃ to probes in NiAl is then given by

$$\frac{f_{23}}{f_{11}} = \frac{1}{A} \left(\frac{x_{11} - x}{x - x_{23}} \right) \exp\left(\frac{S_{23} - S_{11}}{k_B} \right) \exp\left(-\frac{E_{23} - E_{11}}{k_B T} \right), \quad (1)$$

in which A is the ratio of the number of probe substitution sites in the two phases, x is the sample's Ni-composition, x_{11} and x_{23} are the Ni-compositions at the NiAl and Ni₂Al₃ phase boundaries, and S_{23} and S_{11} are the changes in vibrational entropy that accompany indium substitutions. The quantity $(x_{11} - x)/(x - x_{23})$ is the volume fraction of Ni₂Al₃ given by the lever rule. Note that even when $E_{23} = E_{11}$ and $S_{23} = S_{11}$, the ratio f_{23}/f_{11} differs from the ratio of volume fractions by the geometric factor A . For example, if indium substitutes at both inequivalent aluminum sites in Ni₂Al₃, $A = 5/6$ (1/2 divided by 3/5). The x_{11} and x_{23} in eq. 1 are macroscopic phase boundaries; thus, eq. 1 does not incorporate embryo nucleation. In the event of Ni₂Al₃ embryo nucleation in the NiAl phase field, the ratio f_{23}/f_{11} would be greater than zero for $x > x_{11}$, counter to eq. 1.

Perturbed angular correlation of gamma rays (PAC) is sensitive to the local atomic arrangements found around radioactive probe atoms. The technique allows measurement of the interaction between the nuclear quadrupole moment of the probe and the local electric field gradient (efg) caused either by a non-cubic lattice or by nearby defects. Based on the phase boundaries from Taylor and Doyle [1], analysis of room temperature PAC measurements made in the two-phase field indicated that the fraction of In found in Ni₂Al₃ was larger than its volume fraction [5]. The observation has four possible explanations: (1) indium substitutes with an energy E_{23} in the Ni₂Al₃ phase lower than the energy E_{11} in the NiAl phase, (2) the prefactor $\exp((S_{23} - S_{11})/k_B)/A$ is significantly greater than unity, (3) indium attracts vacancies and nucleates Ni₂Al₃ phase embryos within the NiAl phase, and/or (4) the true phase boundaries lie higher in Ni content. The present study provides measurements at elevated temperatures to help distinguish between these alternatives.

2. Experiment

100-mg samples of Ni–Al were prepared by arc melting foils of 99.999% metal purity with carrier-free ^{111}In under Ar. The fractional concentration of indium was only about 10^{-8} . Samples were annealed at 1050 °C under H_2 for one hour. Compositions were determined from the masses of the foils before arc-melting. Minor mass loss occurred during the melting process and typically leads to an uncertainty of ± 0.1 at.% Ni. At each temperature, samples were allowed to equilibrate for 1 hour before starting a measurement. A measurement at each temperature lasts a few days, allowing additional time for samples to reach thermal equilibrium during measurement. When adjusting from high to low measurement temperatures, the cooling rate was typically 2 °C/min. Measurements were made at temperatures up to 1050 °C using a PAC spectrometer with four BaF_2 detectors at angles of 90° . The result of a PAC measurement is a time-dependent perturbation function $G_2(t)$. More details regarding PAC, the spectrometer, and data reduction may be found in ref. [6].

3. Determination of site-fractions

Ni_2Al_3 and NiAl each have characteristic perturbation functions $G_2(t)$. Fig 1 shows spectra for Ni_2Al_3 and Ni-poor NiAl near its phase boundary. The quadrupole interaction that leads to the observed spectrum for Ni_2Al_3 arises because indium atoms sit at Al lattice sites, which have non-cubic, 3-fold axes of charge symmetry. The NiAl spectrum is comprised of signals from quadrupole interactions between indium atoms and different complexes involving vacancies. Details of all the above quadrupole interactions are found in ref. [5]. Within the two-phase field, the perturbation function should be a weighted sum of the two $G_2(t)$ functions. By fitting spectra to a superposition of the two perturbation functions, one determines the site-fractions f_{23} and f_{11} from the relative $G_2(t)$ signal amplitudes.

Typical PAC spectra from within the Ni_2Al_3 -NiAl two-phase field are shown in Fig. 2. The spectra are from a sample with 44.9 at.% Ni measured at 21, 600, 700, and 800 °C. The 800 °C spectrum is dominated by the signal characteristic of the NiAl phase. The 600 °C spectrum contains a significant Ni_2Al_3 signal in addition to the NiAl signal, and the 700 °C spectrum shows a transition between the signals at 800 and 600 °C. This sequence shows that most of the indium is in the NiAl phase at 800 °C, and as the temperature is lowered, more and more indium is observed to be in the Ni_2Al_3 phase. At 21 °C, the relative fraction of indium in the two phases is about the same as at 600 °C. With respect to the 600 °C spectrum, the 21 °C data appear shifted down and the initial peak that is at about 25 ns is smaller; however, the relative fractions of indium in the two phases are the same at both temperatures. At elevated temperature, vacancies “evaporate” away from the indium probe in NiAl, and the difference between the spectra at 600 °C and 21 °C comes from a corresponding change in the fractions of indium-vacancy complexes.

Site-fractions of Ni₂Al₃ determined from fits of PAC spectra are shown in Fig. 3 superimposed on a portion of the Ni-Al phase diagram. Uncertainties in the indicated f_{23} are about 3% near the NiAl boundary and about 10% near the Ni₂Al₃ boundary. For reference, boundaries of the Ni₂Al₃-NiAl two-phase field as determined by Nash *et al.* [7] are drawn in Fig. 3 as curves.

4. Discussion

The Ni₂Al₃ PAC signal is observed well within the NiAl single-phase field determined by Nash *et al.* at elevated temperature. One possible explanation for this observation is that indium nucleates embryos of Ni₂Al₃; however, since other boundaries that are located higher in Ni content have been reported, another possible explanation is that the NiAl phase boundary in Fig. 3 is incorrect.

4.1. Phase boundary determination assuming that embryos did not form

As an exercise, one can determine the phase boundaries from the PAC site-fraction data. This was done in two different ways. The first method determines the NiAl boundary at fixed composition by considering temperature variation of the data. The second method determines both boundaries simultaneously by fitting the composition dependence of f_{23} at fixed temperature

For each sample with compositions between 43.6 and 45.5 at.% Ni, f_{23} decreases as temperature increases, and the first method extrapolates this trend to determine the NiAl boundary. At the NiAl phase boundary $f_{23}=0$, or $f_{23}/f_{11}=0$. As given in eq. 1, the temperature dependence of the ratio f_{23}/f_{11} is steeper near the NiAl boundary than is the dependence of f_{23} ; therefore, the ratio is used to determine the NiAl boundary from temperature dependence of the PAC data. Ratios are plotted versus temperature in Fig. 4 for samples with 43.6, 44.9 and 45.5 at.% Ni. f_{23}/f_{11} appears to be independent of temperature below 600 °C for 44.9 and 45.5 at.% Ni and independent of temperature below 700 °C for 43.6 at.% Ni. This suggests that equilibrium might not be established between the phases at those temperatures. Linear fits, solid lines shown in Fig. 4, of the ratios that show a change in temperature were made to extrapolate the data to $f_{23}/f_{11}=0$. The extrapolated values indicate that the NiAl boundary should be at 960, 860, and 740 °C for samples with 43.6, 44.9 and 45.5 at.% Ni respectively.

In the second method, the composition trend of f_{23} at each temperature is fitted to determine the Ni₂Al₃ and NiAl phase boundaries. The site-fractions are normalized to unity; thus

$$f_{23} = \frac{f_{23}}{f_{11} + f_{23}} = [1 + f_{11} / f_{23}]^{-1}. \quad (2)$$

Substituting eq. 1 into eq. 2 yields

$$f_{23} = \left[1 + A \frac{(x - x_{23})}{(x_{11} - x)} \exp\left(\frac{S_{11} - S_{23}}{k_B}\right) \exp\left(-\frac{E_{11} - E_{23}}{k_B T}\right) \right]^{-1}. \quad (3)$$

Equation 3 contains many parameters. The simplest possible assumptions were made: indium substitutes in both Al-sites in Ni_2Al_3 ($A=5/6$), and indium does not segregate to one phase or the other ($E_{11}=E_{23}$ and $S_{11}=S_{23}$). The f_{23} data for samples between 43.6 and 45.5 at.% Ni at 600, 700 and 800 °C are shown in Fig. 5. The curves in Fig. 5 result from fits of the f_{23} using equation 3 with x_{23} and x_{11} as free parameters. Fits were also performed on the 21, 300, and 500 °C data but the data and fit results are not shown in Fig. 5 for clarity.

The phase boundaries determined from the PAC data are shown in Fig. 6. The circles are boundary points obtained by extrapolating f_{23}/f_{11} to zero (first method above). The squares are the x_{23} and x_{11} obtained by fitting equation 3 to f_{23} (second method) with white bars indicating the standard deviation of the fitted boundaries. The black bars are the result of a sensitivity analysis of the fitted boundaries to the specified prefactor $A \exp((S_{11}-S_{23})/k_B)$. There is uncertainty from the PAC measurements as to whether indium substitutes on both Al sublattices or on only one Al sublattice in Ni_2Al_3 . Lacking knowledge about S_{11} and S_{23} , and supposing that indium might substitute at only one Al-site in Ni_2Al_3 , the prefactor could change by a factor of 2. The ends of the black bars in Fig. 6 correspond to fits of f_{23} by method 2 in which the prefactor 5/6 was varied by a factor of two.

4.2. Comparison of phase boundaries

Fig. 6 also shows three recent sets of boundaries from the literature. Boundaries that were determined by fitting f_{23} according to equation 3 are in closest agreement with the Kek boundaries [8], which lie at the highest Ni-compositions of the three sets. The boundaries from Nash *et al.* [7] are lower in Ni-composition and are largely based on the data of Taylor and Doyle [1] and Ellner, Kattner and Predel [9]. Okamoto's boundaries [10] are located at intermediate compositions. The disagreement between the Kek and Nash boundaries may be explained by differences in sample preparation. The Kek boundaries come from a phase diagram that includes Ni_3Al_4 . The formation of Ni_3Al_4 is very sluggish and takes 127 days to equilibrate at 560 °C [11]. In contrast, the Nash boundaries are based on measurements in which samples were allowed to equilibrate for from 30 minutes to 2 days. The samples used in this PAC study were equilibrated for 1 hour prior to measurement and continued to equilibrate for a few days while spectra were collected. Table 1 summarizes the preparation of samples used to determine the boundaries illustrated in Fig. 6.

5. Conclusion

Based on preparation conditions, the samples in our study should be more like those from which the Nash boundaries are derived. Therefore, because the Ni_2Al_3 signal is observed well within the NiAl single-phase field of the Nash boundaries (and even the Okamoto boundaries), it is concluded that isolated indium solute atoms can nucleate embryos of Ni_2Al_3 within the single-phase field of NiAl.

Acknowledgement

This work was supported in part by the National Science Foundation under grant DMR 96-12306 (Metals Program).

References

-
1. A. Taylor, N.J. Doyle, *J. Appl. Cryst.* 5 (1972) 201.
 2. J. Fan, S. Collins, *Hyperfine Interactions* 60 (1990) 60.
 3. G.S. Collins, J. Fan, B. Bai, in: M.V. Nathan et al. (Eds.), *Structural Intermetallics, The Minerals, Metals and Materials Society*, 1997, p. 43.
 4. B. Bai, G.S. Collins, in: E.P. George, M. Mills, M. Yamaguchi, *High-temperature ordered intermetallic alloys VIII, Materials Research Society Symposium Proceedings* 552 (1999) 541.
 5. G.S. Collins, L. S.-J. Peng, M.O. Zacate, *Z. Naturforschung* 55a (2000) 129.
 6. G.S. Collins, S.L. Shropshire, J. Fan, *Hyperfine Interactions* 62 (1990) 1.
 7. P. Nash, M.F. Singleton, J.L. Murray, in: *Phase Diagrams of Binary Nickel Alloys*, ASM International, 1991, p. 3.
 8. T. Goedecke, M. Ellner, *Z. Metallkd.* 88 (1997) 5; Reference 24.
 9. M. Ellner, U. Kattner, B. Predel, *Journal of Less-Common Metals* 87 (1982) 305.
 10. H. Okamoto, *Journal of Phase Equilibria* 14 (1993) 257.
 11. M. Ellner, S. Kek, B. Predel, *Journal of Less-Common Metals* 154 (1989) 207.

Table 1. Equilibration times of samples used to determine the Ni_2Al_3 -NiAl two-phase boundaries

Study	Sample equilibration time	Reference
present	1 hour – few days	--
Nash <i>et al.</i>	30 min. – 2 days	[1, 9]
Okamoto	30 min. – 2 days	[10]
Kek	127 days	[11]

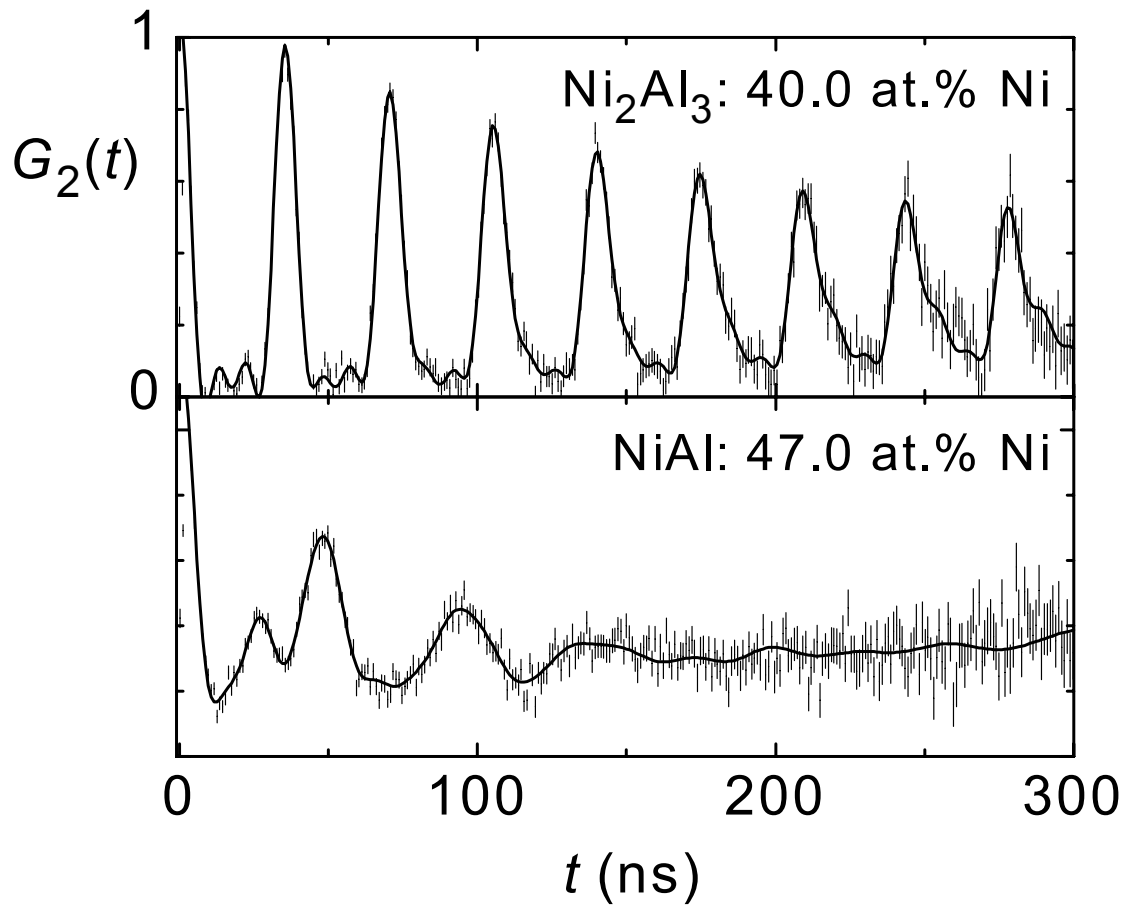


Fig. 1. PAC spectra of Ni₂Al₃ and Ni-poor NiAl. The observed patterns are signatures of each phase in the two-phase field between ~42 and ~46 at.% Ni.

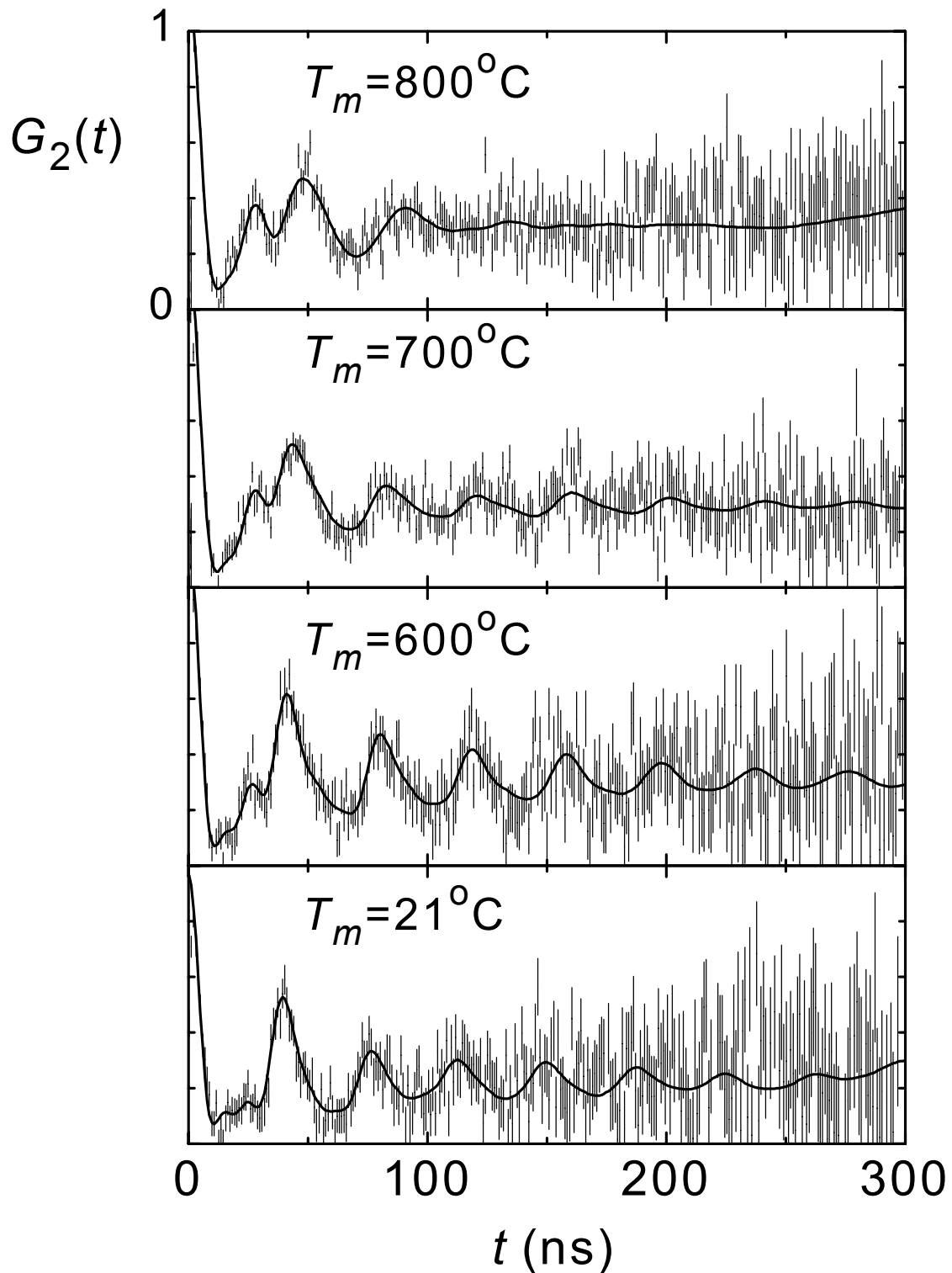


Fig. 2. PAC spectra of Ni-Al with 44.9 at.% Ni measured at the indicated temperatures. The site fractions of indium probes in the Ni_2Al_3 and NiAl phases are observed to change with temperature (compare Fig. 1).

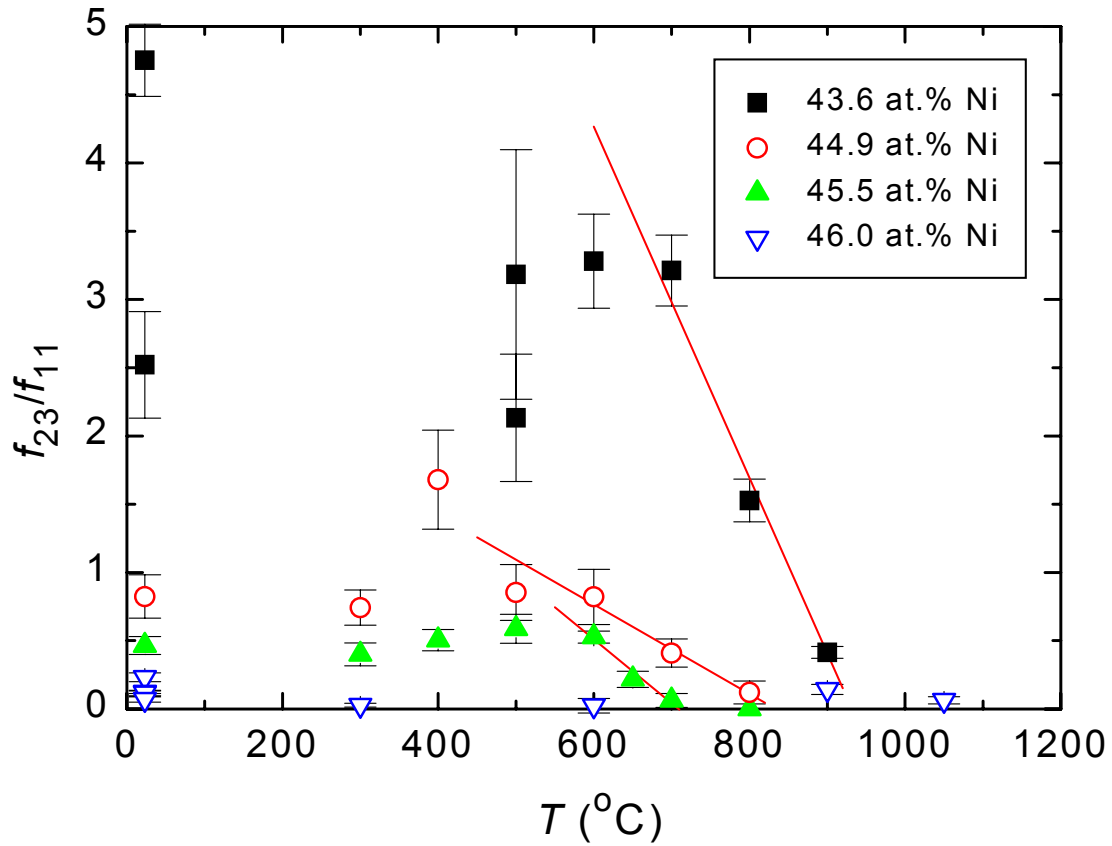


Fig. 4. Ratio of site-fractions of indium probes in Ni_2Al_3 to NiAl phases of four Ni-Al samples as a function of temperature. The straight lines are linear fits to determine the NiAl phase boundary, for which $f_{23}/f_{11}=0$.

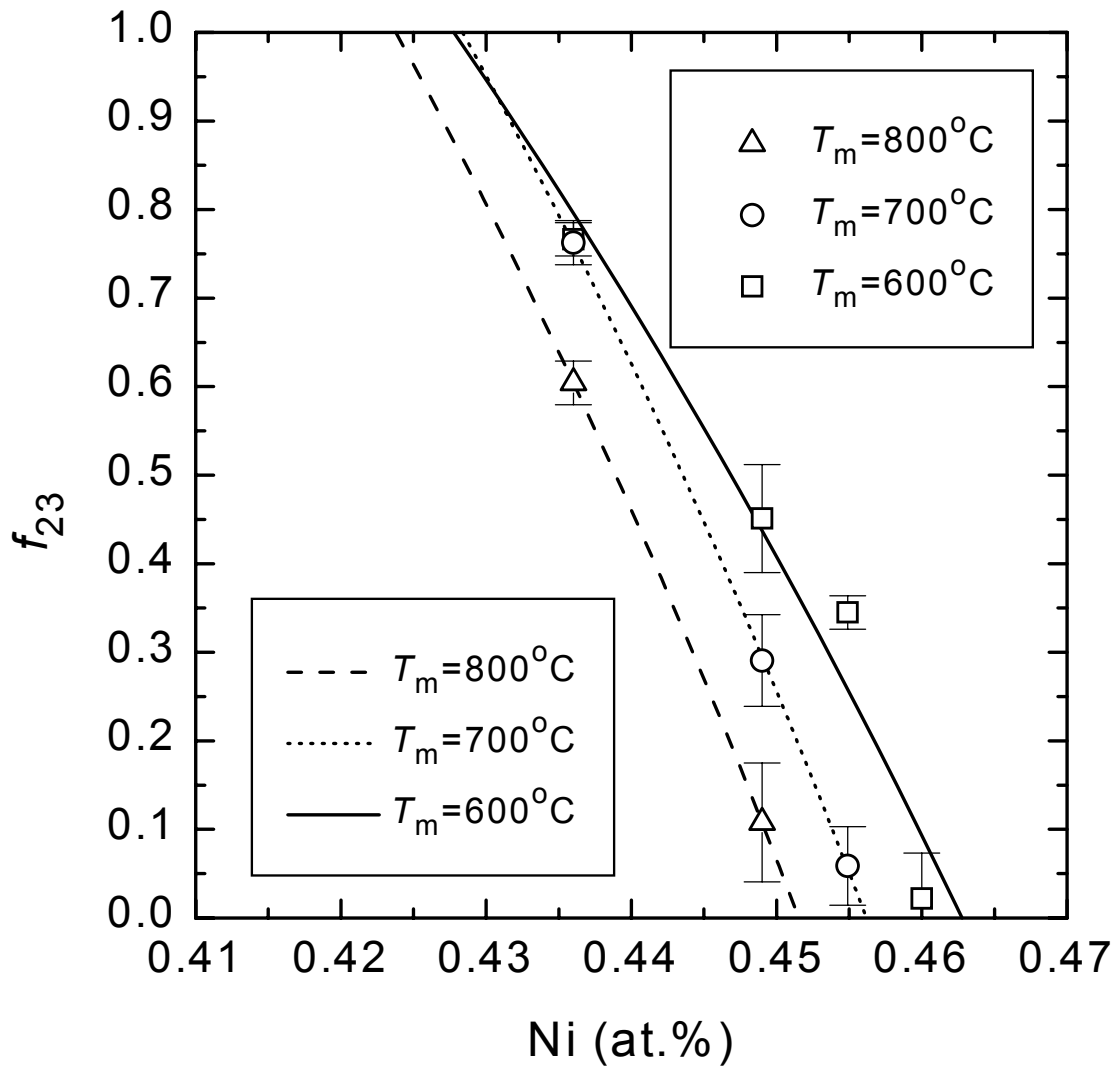


Fig. 5. Site-fractions of the Ni_2Al_3 phase at three temperatures as a function of composition. The curves show fits using equation 3 with $A=5/6$. The boundaries x_{23} are located where $f_{23}=1$ and the x_{11} are located where $f_{23}=0$. (Other temperature data are omitted for clarity.)

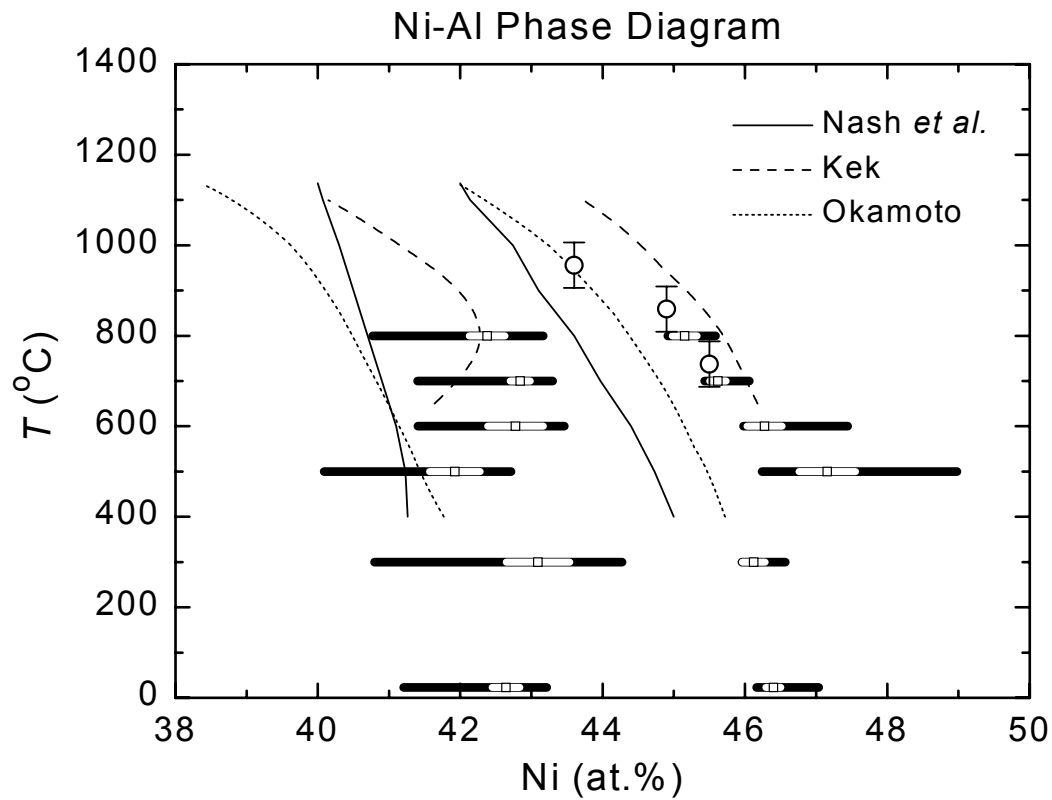


Fig. 6. Portion of the Ni-Al phase diagram between 38 and 50 at.% Ni. Phase boundaries fitted from Fig. 4 are shown as circles. Phase boundaries fitted as in Fig. 5 are shown by horizontal bars. The inner unfilled bars give uncertainties using $A=5/6$. The outer bars show the range of fitted boundaries when A is varied between $5/3$ and $5/12$. Also shown as curves are published phase boundaries by Nash et al. [7] (solid), Kek [8] (dashed), and Okamoto [10] (dotted).